Biogeosciences, 21, 5045–5057, 2024
https://doi.org/10.5194/bg-21-5045-2024

Biogeosciences Open Access EGU

Anticorrelation of net uptake of atmospheric CO_2 by the world ocean and terrestrial biosphere in current carbon cycle models

Stephen E. Schwartz

School of Marine and Atmospheric Sciences, Stony Brook University, Stony Brook, NY 11794, USA

Correspondence: Stephen E. Schwartz (stephen.schwartz@stonybrook.edu)

Received: 13 March 2024 – Discussion started: 22 May 2024
Revised: 9 September 2024 – Accepted: 13 September 2024 – Published: 15 November 2024

Abstract. The rate at which atmospheric carbon dioxide (CO_2) would decrease in response to a decrease in anthropogenic emissions or cessation (net zero emissions) is of great scientific and societal interest. Such a decrease in atmospheric CO_2 on the centennial scale would be due essentially entirely to transfer of carbon into the world ocean (WO) and the terrestrial biosphere (TB), which are sink compartments on this timescale. The rate of decrease in excess atmospheric CO_2 and the apportionment of this decrease into the two sink compartments have been examined in two prior model intercomparison studies, subsequent either to a pulse emission of CO_2 or to abrupt cessation of anthropogenic CO_2 emissions. The present study examines and quantifies inter-model anticorrelation in those studies in the net rate and extent of uptake of CO_2 into the two sink compartments. Specifically, in each study the time-dependent coefficients characterizing the net transfer rate into the two sink compartments (evaluated as the net transfer rate normalized to excess atmospheric CO_2 above the pre-pulse amount for the pulse experiment or as the net transfer rate divided by excess atmospheric CO_2 above the preindustrial amount for the abrupt cessation experiment) were found to exhibit strong anticorrelation across the participating models. That is, models for which the normalized rate of uptake into the WO was high exhibited low uptake rate into the TB and vice versa. This anticorrelation in net transfer rate results in anticorrelation in net uptake extent into the two compartments that is substantially greater than would be expected simply from competition for excess CO_2 between the two sink compartments. This anticorrelation, which is manifested in diminished inter-model diversity, can lead to artificially enhanced confidence in current understanding of the consequences of potential future reductions of CO_2 emissions and in the global warming potentials of non-CO_2 greenhouse gases relative to that of CO_2.

1 Introduction

Essentially, the only means by which excess carbon dioxide (CO_2), i.e., above its preindustrial level, is removed from the atmosphere on the centennial scale is net uptake by the world ocean (WO) and the terrestrial biosphere (TB). Here the term net uptake is used to emphasize that transfer of CO_2 from the atmosphere to these two compartments of Earth's biogeosphere is highly reversible; hence it is this net transfer that is pertinent to the disposition of excess atmospheric CO_2 due to anthropogenic emissions on this timescale. Historically, over the industrial era, the increase in atmospheric CO_2 has been about half of anthropogenic emissions (Bacastow and Keeling, 1973; Friedlingstein et al., 2022). Hence the processes governing this net uptake, as well as the model-based representation of these processes, are of great scientific and societal interest. The need for confident understanding and model-based representation of these processes has become increasingly acute because of the societal need to assess the consequences of prospective reduction or cessation (net zero emissions) of anthropogenic CO_2 emissions and to develop effective strategies to achieve specified targets, such as the mixing ratio of atmospheric CO_2 or the increase in global temperature.

Briefly, net drawdown of excess CO_2 (above its preindustrial level) from the atmosphere to the ocean consists of a highly reversible exchange of CO_2 between the atmosphere and the upper ocean, resulting in increased concentration of dissolved inorganic carbon (DIC) in the upper ocean over time relative to its preindustrial value, followed by largely irreversible net transfer of DIC from the upper ocean to the deep ocean associated with water mass exchange from the upper ocean to the deep ocean. Similarly, uptake of excess CO_2 from the atmosphere to the terrestrial biosphere consists

of rapid exchange of carbon between the atmosphere and the TB in association with increased photosynthesis and respiration due to increased atmospheric CO_2, with a small fraction of the increased carbon stock in the TB being taken up by long-lived woody and soil components of the TB. An accurate representation of these processes is the objective and a requirement for models of varying degrees of complexity that are to be used in the assessment of the response of atmospheric CO_2 to potential future changes in CO_2 emissions.

A key means of assessing current understanding and model-based representation of processes governing the drawdown of atmospheric CO_2 in carbon cycle models is model intercomparison studies, more specifically a comparison of the modeled response of the change of the amount of carbon in the atmosphere, the WO, and the TB in response to a perturbation in emissions. (A perturbation in emissions is required because, in the absence of such a perturbation, the carbon stocks in the three compartments would be in a steady state, i.e., not changing.) Such intercomparison studies are intended to reveal, through inter-model diversity in model response, the extent to which model-based representations of the processes governing net uptake of CO_2 differ among the participating models and thus to serve as a measure of uncertainty in understanding. In principle as well, such intercomparisons might reveal reasons for differences among the models and lead to improvement in areas of disagreement.

In this study attention is directed to two key model intercomparison studies that examined changes in carbon stocks in the three compartments (atmosphere, WO, and TB) following abrupt changes in CO_2 emissions. The three compartments are considered a closed system; consequently, the net change in atmospheric CO_2 subsequent to the pulse (or cessation) is the complement of the net changes in carbon stocks of the other two compartments. Joos et al. (2013; hereinafter J13) reported the disposition of a pulse emission of CO_2 with a magnitude of 100 Pg C emitted into the atmosphere as the amount of increase in carbon in each of the three compartments as a function of time subsequent to the emission pulse, thereby obtaining impulse response functions (IRFs; fraction of emitted pulse in each compartment as a function of time subsequent to the pulse) for each of the three compartments. MacDougall et al. (2020; hereinafter M20) examined the decrease in atmospheric CO_2, as well as the net uptake into the WO and the TB, subsequent to the abrupt cessation of anthropogenic CO_2 emissions (ZECMIP study, Zero Emissions Commitment Model Intercomparison Project). The two studies are not wholly independent in that several models or modeling groups participated in both intercomparisons.

Because these two studies reported not only the decrease in atmospheric CO_2 but also net uptake of carbon by the WO and the TB, it is possible to assess inter-model diversity not only in the decrease in atmospheric CO_2 but also in the net changes in the carbon stocks in the other two compartments in response to the perturbation in emissions, as governed by the process represented in the models. Here it should be noted that some inherent anticorrelation across the models is expected in the extent of uptake into the WO and the TB; because the WO and the TB are the only sinks of atmospheric CO_2, a greater uptake into one compartment would necessarily result in a lower uptake into the other. In contrast, the transfer coefficients characterizing the net uptake of atmospheric CO_2 into the WO and the TB, defined as the time-dependent net rate of uptake into the compartment divided by the time-dependent amount of excess atmospheric CO_2, would be expected to be uncorrelated if treatment of the processes governing the net uptake rate into one compartment were independent of that governing the net uptake rate into the other compartment across the set of models participating in the studies. Here the inter-model correlations in extent and rate of uptake of atmospheric CO_2 are examined to assess the independence of the representation of uptake of atmospheric CO_2 into the WO and the TB in the models participating in each of the two intercomparison studies. Any substantial negative correlation transfer coefficients representing uptake of atmospheric CO_2 into the two compartments would be indicative of compensating effects, whereby models having a net uptake rate into one compartment have a higher net uptake rate into the other, thereby resulting in a reduced inter-model diversity in the rate and extent of decrease in atmospheric CO_2. As inter-model diversity is commonly taken as a measure of uncertainty, any such negative correlation would artificially reduce the perceived uncertainty in the rate of drawdown of excess atmospheric CO_2 subsequent to a perturbation.

2 Analysis and findings

2.1 Joos et al. (2013)

J13 examined the decrease in atmospheric CO_2 and the integrated net flux from the atmosphere into the ocean and into the TB subsequent to a 100 Pg C emission pulse added to an atmosphere having a prior CO_2 mixing ratio of 389 ppm. The extent of decrease was reported as the difference between the run with the 100 Pg pulse and a reference run with mixing ratio held constant at 389 ppm. Participating models were three comprehensive Earth system models (ESMs), seven Earth system models of intermediate complexity (EMICs), and four box-type models. The disposition of excess atmospheric carbon was presented graphically as IRFs, the fractions of the emitted pulse in the atmosphere, the ocean, and the TB over two time periods: 0.5 to 100.5 years subsequent to the pulse and 100.5 to 1000.5 years. In this analysis results are examined only for the first 100 years, over which time the excess atmospheric stock resulting from the pulse decreased by about 60 %. The J13 study has assumed considerable importance because its multimodel mean is widely used for evaluation of the consequences of prospective future profiles of CO_2 emissions and for comparison of integrated

radiative forcing of non-CO_2 greenhouse gases with that of CO_2 (so-called greenhouse warming potentials; e.g., Myhre et al., 2013, IPCC Fifth Assessment Report). The results of the J13 study have also been used to represent the response to pulse emission of CO_2 in simple climate emulators such as the widely used FAIR (Finite Amplitude Impulse-Response) climate emulator (Millar et al., 2017; Smith et al., 2018).

The time dependence of the IRFs for the several compartments over the 100-year time period following pulse emission (Fig. 1a) shows that each model exhibited a monotonic or nearly monotonic net increase in the ocean IRF over this period, with the IRFs of the several models relatively smooth over the time period. In contrast several of the models exhibited substantial fluctuations in extent of net uptake into the TB (Fig. 1b); a negative derivative denotes a temporary negative net flux, i.e., net flux from the TB to the atmosphere. The atmospheric IRFs, nominally the complements of the sums of the ocean and the TB IRFs, exhibited fluctuations more or less comparable to those of TB IRFs for the several models; here a positive slope denotes a temporary increase in atmospheric stock. Comparison of the inter-model diversity of the IRFs (as shown by the ranges of pink shading in Fig. 1a, b, and c denoting ± 2 SD) on the same vertical scale for the several IRFs demonstrates that the inter-model diversity of the atmospheric IRFs (Fig. 1c) is systematically and substantially lower than that for the TB. As the decrease in the atmospheric stock is the sum of the uptakes into the ocean and TB compartments, the variance across the models of the atmosphere IRFs would, if uptake into the ocean and TB were uncorrelated across the models, be expected to exceed the variance for both the ocean and TB IRFs. The contravention of that expectation must therefore be due to anticorrelation of the IRFs across the models. This anticorrelation is examined further in Fig. 1d by means of the regression slope of IRF(WO) vs. IRF(TB), which is negative throughout essentially the entire 100-year time period, approaching -0.4 by the end of the time period, with the difference from the value 0, which would be expected in the absence of anticorrelation of the regression slope, up to severalfold greater than the SD of that slope obtained from the linear least-squares regression. (Throughout this study correlation coefficients, regression coefficients, and their uncertainties are calculated by the linear regression model, as described, e.g., by Press et al., 1997.) The anticorrelation is examined further in Fig. 1e, which shows the Pearson r correlation coefficient to be negative throughout the time period, approaching -0.9 at the end of the time period, again indicative of strong anticorrelation of IRF(WO) and IRF(TB) across the set of models that participated in this intercomparison study.

What are the causes of the anticorrelation? It would seem that there are two potential contributions to this. The first would be competition between the two sinks for the excess atmospheric CO_2 remaining from the pulse at a given time subsequent to the pulse; if, at a given time, more of this excess CO_2 had previously been drawn down into one compartment, there would be less CO_2 available to be drawn down into other compartment, resulting in anticorrelation in the amounts in the two compartments simply because of this competition effect. A second, more intrinsic and concerning source of anticorrelation would be compensating treatments in the several models of the processes that govern the uptake of the excess CO_2 from the pulse emission by the WO and the TB such that if the rate of uptake into the WO in a given model were high relative to the other models, the rate of uptake into the TB would be low and vice versa.

An example of the anticorrelation across the suite of models between the IRFs for uptake into the ocean and the TB is shown in Fig. 2a for time subsequent to pulse injection (time $t = 99.5$ years). This example likewise shows strong anticorrelation, with models exhibiting high uptake into the ocean exhibiting, low uptake into the TB, and vice versa. The Pearson r coefficient is negative, with a value of -0.85, and r^2, the fraction of the variance in the relation between IRF(WO) and IRF(TB) accounted for by the regression, is 0.72. The standard deviations of the IRFs obtained with the several models at $t = 99.5$ years are 0.061 and 0.118, respectively, much greater for the TB than for the ocean, as shown also in Fig. 1a and b. Using these values for σ_O and σ_T yields an unbiased estimate of σ_A at $t = 99.5$ years, evaluated as the quadrature sum, $\sigma_A = \left(\sigma_O^2 + \sigma_T^2\right)^{1/2} = 0.132$, nearly twice the value obtained from the modeled atmospheric IRFs themselves, 0.071.

Assessment of whether, and to what extent, the anticorrelation is due to the treatment of the processes versus due simply to competition requires examination of the rates of transfer of excess CO_2 as a function of time subsequent to the pulse rather than of the IRFs themselves, which are the integrals of the transfer rates. The IRFs would be subject to the competition effect, whereas the time-dependent transfer rates would not. Hence, to assess the extent to which the anticorrelation is due to the competition effect, a similar analysis was conducted of the coefficients characterizing the rate of net transfer of excess CO_2 from the atmosphere into each of the sink compartments. To this end the net transfer coefficients into the ocean and the terrestrial biosphere were evaluated as the rate of net uptake of CO_2 (reckoned as C) into the specific compartment (WO or TB) per excess stock remaining in the atmospheric compartment at a given time:

$$k_O = \frac{\mathrm{d}f_O/\mathrm{d}t}{f_A} \text{ and } k_T = \frac{\mathrm{d}f_T/\mathrm{d}t}{f_A}, \quad (1)$$

respectively, where f_O and f_T denote the time-dependent impulse response functions (IRFs) of the two compartments, and f_A similarly denotes the time-dependent IRFs of the atmospheric stock, all expressed as fractions f of the carbon mass of the emitted pulse. Dividing the time-dependent net transfer rates ($\mathrm{d}f_O/\mathrm{d}t$, $\mathrm{d}f_T/\mathrm{d}t$) by the time-dependent atmospheric IRFs (f_A) to obtain the time-dependent net transfer coefficients (k_O, k_T) results in quantities that would be constant if the net fractional uptake rate of excess CO_2 exhib-

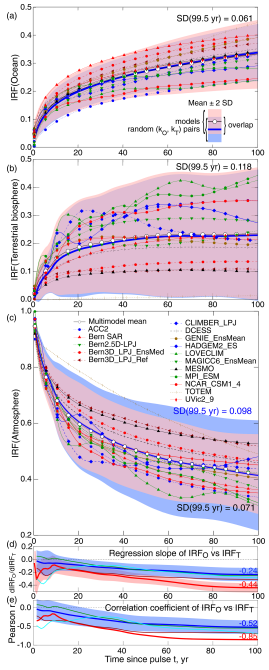

Figure 1. Time-dependent impulse response functions (IRFs, f) for the perturbations in stocks in **(a)** the world ocean f_O, **(b)** the terrestrial biosphere f_T, and **(c)** the global atmosphere f_A, as a function of time t subsequent to the emission of a 100 Pg(C) pulse of CO_2 into the atmosphere, in excess of the amount of carbon that would be present in each compartment for atmospheric CO_2 held constant at the value at the time of emission of the pulse, as calculated by the models that participated in the model intercomparison study of Joos et al. (2013, J13). For details on the intercomparison and identification of the models, see J13. The three panels are to the same scale. Adapted from Joos et al. (2013), line codes and symbol shapes are as in J13. Pink shading denotes ± 2 SD, about the multimodel mean. SDs at $t = 99.5$ years after the pulse are in black text. The thick blue curve and blue shading denote the mean and ±2 times the mean SD of 120 instances of IRFs calculated with randomly sorted pairs of net transfer coefficients (k_O, k_T) taken from the sets of net transfer coefficients evaluated from the data presented by J13. Mean SD for f_A at $t = 99.5$ years is in blue text in **(c)**. The key at the lower right of **(a)** shows mean (black, white markers) ±2 SD for models (pink shading), mean (thick dark blue) ±2 SD (light-blue shading) for randomly sorted (k_O, $k_{T,i}$) pairs, and region of overlap (violet shading). Attention is called to slight non-overlapped regions in *a* and *b* and a large non-overlapped region in **(c)**. **(d)** Thick red lines indicate the regression slope of linear fit of f_O vs. f_T among the models for each year over the 100-year period subsequent to pulse emission (example shown in Fig. 2); pink shading denotes estimated error in slope as obtained from the regression (±1 SD); thick blue lines indicate the mean of the regression slope of the linear fit of f_O vs. f_T evaluated for 120 instances of randomly sorted (k_O, $k_{T,i}$) pairs; blue shading denotes ±1 SD of these 120 instances; thin curves denote time series of regression slopes for three instances of such random pairings. **(e)** Pearson correlation coefficient r of the regression of f_O vs. f_T for the several models (thick red); thick blue and blue shading are the mean and SD of r for 120 instances of IRFs, as in **(d)**. Thin curves denote correlation coefficients for three instances of those regressions.

ited a constant proportionality to the amount of excess CO_2, much like a rate constant for a first-order reaction in chemical kinetics. The departures from constancy in k_O (Fig. 3a) and to much greater extent in k_T (Fig. 3b) are manifestations of the effects of the history of prior uptake of CO_2 by the two compartments and of the time-dependent states of these compartments affecting this net uptake.

Similarly, the coefficient denoting the net rate of decrease in the IRFs for stock in the global atmosphere is given by

$$k_A = -\frac{\mathrm{d}f_A/\mathrm{d}t}{f_A}; \tag{2}$$

the derivatives were calculated numerically from the IRFs presented by J13. (As the figures of J13 were published as vector graphics, it was possible to digitize the data quite precisely; the data are also tabulated at https://climatehomes.unibe.ch/~joos/IRF_Intercomparison/, last access: 31 October 2024) The results of this examination are presented in Fig. 3 as a function of time subsequent to the pulse and in Fig. 2b for a single value of time. At first glance, the transfer coefficients plotted similarly to the IRFs are similar to the IRFs themselves. However the values of the k's, being proportional to the derivatives of the IRFs, exhibit much greater fluctuations than the IRFs themselves (especially k_T), some being rather smooth and others exhibiting rather large, high-frequency fluctuations. A local maximum in an IRF results in a change in sign (from positive to negative) in the net transfer coefficient: a net transfer of excess CO_2 resulting from the emission pulse being transferred thereafter from the WO or the TB back to the atmosphere and correspondingly a local minimum in the IRFs, resulting in a change in sign in the transfer coefficient from negative to positive. Essentially, no such return transfer from the ocean to the atmosphere is exhibited by the any of the models (very slight return transfer for two of the models); in contrast, all but three of the models exhibited return flux from the TB to the atmosphere at one or more times in the 100-year period examined (Fig. 3b), with two of the models exhibiting instances of return flux of greater than 1 % yr^{-1} relative to the amount of remaining excess atmospheric stock. As with the IRFs themselves, the anticorrelation between the transfer coefficients k_O and k_T is demonstrated graphically by the narrower spread of k_A than k_T; Fig. 3a–c are drawn to the same scale. Quantitatively, as manifested by the traces for regression slope and correlation coefficient, throughout the time over which the two compartments were drawing down the major fraction of the pulse-emitted CO_2, roughly the first 60 years or so subsequent to the pulse (Fig. 1c), there is again systematic anticorrelation, here between k_O and k_T (negative of Pearson r as great as 0.88). An example of time $t = 50.5$ years subsequent to the pulse (Fig. 2b) shows a quite strong anticorrelation in the transfer coefficients into the WO and the TB across the models, $r^2 = 0.72$. This anticorrelation in the transfer coefficients themselves rules out the anticorrelation in the IRFs as being due solely to the competition effect and demonstrates that for

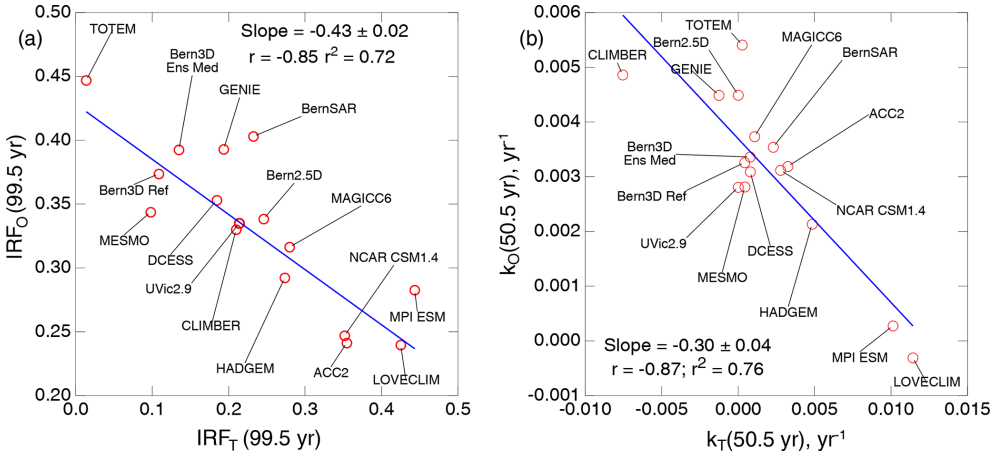

Figure 2. **(a)** IRFs for uptake of excess CO_2 by the world ocean versus those by the terrestrial biosphere, both given as fraction relative to the magnitude of the pulse, at time $t = 99.5$ years subsequent to pulse injection, as represented by the models that participated in the model intercomparison study of Joos et al. (2013, J13). Blue lines denote the linear regression. Also shown are the regression slope, the Pearson correlation coefficient r (the negative value of which denotes anticorrelation), and r^2 (the fraction of the variance that is accounted for by the regression). For identification of models, see J13. **(b)** As in **(a)** but for the transfer coefficient for net uptake of excess CO_2 from the atmosphere to the WO k_O versus that from the atmosphere to the terrestrial biosphere k_T at time $t = 50.5$ years; negative values denote net transfer from the ocean or the TB to the atmosphere at that time.

models for which the transfer rate into the ocean was high relative to the multimodel mean, the transfer rate into the TB was low relative to the multimodel mean and vice versa.

The cause of the anticorrelation of the IRFs was further assessed by calculations of the IRFs in which the k_T's of the several models were randomly paired with the k_O's, with examination of the resultant correlations between IRFs for uptake by the WO and the TB. First, the possibility of any correlation among the random pairs of the time-dependent transfer coefficients was assessed; as anticipated, these random pairings exhibited essentially no correlation. The mean regression slope over the 120 instances was essentially zero over the 100-year period with the mean at $t = 100$ years -0.0009 (Fig. 3d); the mean Pearson r was likewise essentially zero, with a standard deviation of about 0.25 over the time range, and with a mean at $t = 100$ years -0.003 (Fig. 3e). To be sure there was meandering of both quantities for individual instances of pairing, three instances are shown in Fig. 3d and e, with some of the individual curves meandering considerably outside ± 1 SD, but that is of course to be expected. None exhibited the systematic strong anticorrelation exhibited by IRFs of the models, as shown by the thick red curve, with an $-r$ as great as 0.88 or 3.5 times the SD obtained with the randomly paired k_O and k_T.

To assess the contribution of the competition effect to the anticorrelation in the IRFs themselves, the randomized pairs of time-dependent k_O and k_T were used to calculate time-dependent IRFs corresponding to those randomized (k_O, k_T) pairs. To do this, first the time-dependent IRFs of the atmospheric stock were evaluated for each (k_O, k_T) pair as the integral:

$$f_A(t) = \exp\left(-\int (k_O(t) + k_T(t))\,dt\right). \quad (3)$$

Then the IRFs of the WO and the TB were evaluated for each (k_O, k_T) pair as the integrals of the transfer rates.

$$f_O(t) = \int k_O(t)\, f_A(t) dt \text{ and } f_T(t) = \int k_T(t)\, f_A(t) dt \quad (4)$$

The accuracy of this approach was demonstrated by examination of the IRFs calculated in this way for the original (k_O, k_T) pairs, which closely reproduced the original IRFs. The results of this examination are shown in Fig. 3d for the regression slope and Fig. 3e for the correlation coefficient of f_O vs. f_T over the 100-year period. In each panel the thick red curve denotes the time-dependent quantity evaluated for the (k_O, k_T) pairs of the 16 models of the Joos et al. (2013) study, as described above. The same analysis was then conducted for 120 instances in which a randomly sorted set of transfer coefficients $k_{T,i}$ was paired with the set of transfer coefficients in the Joos et al. (2013) study k_O, and the model was run for 100 years for each randomized pair of transfer coefficients (k_O, $k_{T,i}$); that process was then carried out for a total of 120 runs with randomized pairs (k_O, $k_{T,i}$), $0 \le i \le 119$. The thick blue curve denotes the mean of the respective quantity for the 120 randomized pairs (k_O, $k_{T,i}$), and the blue shading denotes the SD of the respective quantity. (As with the transfer coefficients, the curves for individual (k_O, $k_{T,i}$) pairs meandered about the mean.) The non-zero values of the mean regression slope and the mean correlation coefficient of the IRFs evaluated with the randomized pairs

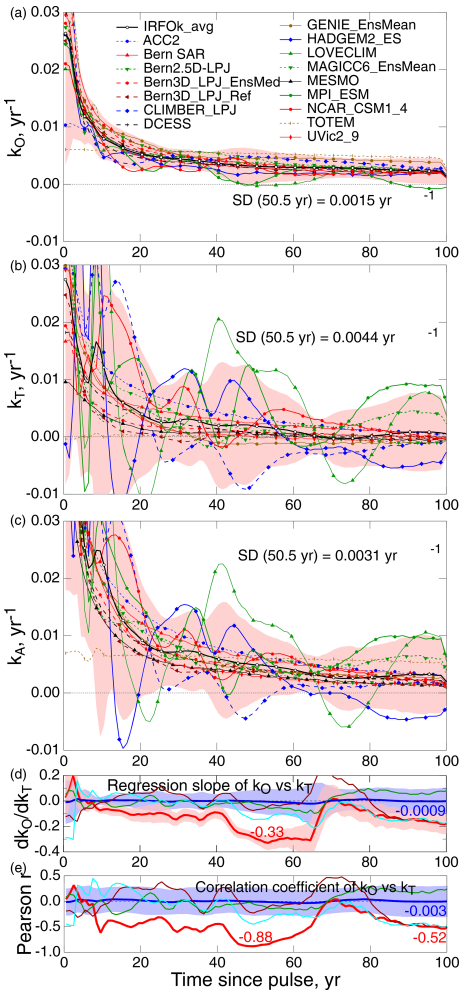

Figure 3. Net transfer coefficients from the atmosphere into **(a)** the world ocean (k_O) and **(b)** the terrestrial biosphere (k_T) as a function of time t subsequent to emission of a 100 Pg(C) pulse of CO_2 into the atmosphere, evaluated from the results from the model intercomparison of Joos et al. (2013); similarly, **(c)** the fractional rate of net decrease in excess CO_2 stock in the atmosphere; negative values denote a temporary net increase. Pink shading denotes ± 2 SD about the multimodel mean; SDs at $t = 50.5$ years are indicated; the three panels are to the same scale. For identification of the models, see J13; line codes and symbol shapes are as in J13. **(d)** Regression slope (thick red line) of the linear fit of k_O vs. k_T for the several models for each year over the 100-year period subsequent to pulse emission (see Fig. 2b for example), with the value at $t = 53.5$ years indicated (red text). Pink shading denotes ± 1 SD. Mean regression slope is denoted by the thick blue line, and ± 1 SD is denoted by blue shading for 120 instances of k_O and k_T of different models being randomly paired, with a mean value at $t = 100$ years indicated (blue text); thin curves denote time series of three instances of those regression coefficients. **(e)** Pearson correlation coefficient r of linear regression of k_O vs. k_T for the several models (thick red), with values at $t = 49.5$ and 99.5 years indicated by red text; blue and blue shading denote the mean and ± 1 SD of r, for 120 instances of k_O and k_T of different models being randomly paired, with the mean value at $t = 100$ years indicated by blue text; thin curves denote time series of three instances of those correlation coefficients.

of transfer coefficients are measures of the competition effect, the negative regression coefficient $-r$ increasing over the 100-year period to 0.52 by the end of that period, a substantial fraction of the value for the models themselves, 0.85. The enhancement of the anticorrelation in IRFs due to anticorrelation of the transfer coefficients may be inferred from the increase in the regression slope of f_O vs. f_T for the original models compared to that for the randomized (k_O, k_T) pairs, a factor of about 1.8.

The effect of anticorrelation between the net transfer coefficients in the models is examined also in Fig. 1a–c, by comparison of the standard deviations of the IRFs of the several compartments for each year up to 100 years following the pulse, as calculated in model runs with 120 instances of the randomized pairs (k_O, $k_{T,i}$) with those of the models themselves. (Here the mean of the IRFs obtained from the integration, which was initiated at time subsequent to the pulse $t = 0$, was set to match the mean of the IRFs presented by J13 at $t = 0.5$ year, the earliest time presented by J13.) The SDs of the IRFs for the WO and the TB for the randomized pairs, shown by the blue shading denoting ± 2 SD about the mean, are essentially identical over the entire 100-year period to the SDs for the models, shown by the pink shading, with nearly complete overlap (purple) between the blue and pink shading and only slight regions of non-overlap – pink toward the tops of the shaded areas in Fig. 1a and b and a slight region of non-overlapped blue toward the bottom of the shaded area in Fig. 3b. However the SD for the IRF of the atmosphere calculated with the randomized pairs (k_O, $k_{T,i}$) is substantially greater than that for the models (Fig. 1c), as manifested by the substantial region of non-overlapped blue extending well above and below the overlap region. The decrease in inter-model spread of the atmospheric IRFs of the models participating in the intercomparison relative to that calculated for random pairing of the transfer coefficients is thus confidently attributed to anticorrelation of the sets of transfer coefficients across the models.

By the several measures presented here, the inter-model spread of the IRFs denoting the decrease in atmospheric CO_2 subsequent to injection of a pulse of CO_2 presented by J13 would seem to be much less than would be expected in the absence of inter-model anticorrelation of the normalized net transfer rates of atmospheric CO_2 to the WO and the TB. This reduction would seem to be due to compensating treatments of the underlying processes that control this transfer such that for models for which k_O was high relative to the multimodel mean, the average value of k_T was low relative to the multimodel mean and vice versa.

2.2 MacDougall et al. (2020)

The ZECMIP model intercomparison study (MacDougall et al., 2020; M20) was similar to that of Joos et al. (2013), except that it examined the drawdown of atmospheric CO_2 (as well as uptake of this atmospheric CO_2 by the world ocean

and terrestrial biosphere) subsequent to an abrupt cessation of emissions rather than in response to a pulse emission. The protocol of the M20 study was that atmospheric CO_2 was forced, in each of the models, to increase from its preindustrial value at 1 % yr^{-1} until cumulative emissions reached 1000 Pg C (by coincidence, atmospheric CO_2 was approximately twice its preindustrial value in most models), at which point anthropogenic emission was abruptly ceased. Participating models were nine ESMs and nine EMICs. The paper itself and the Supplement reported stocks of excess carbon in the atmosphere, the WO, and the TB and net transfer rates from the atmosphere to the WO and the TB subsequent to the cessation. Results from that study are examined here similarly to the examination of the results from the study of J13. Data were obtained from the Supplement of M20 and at http://terra.seos.uvic.ca/ZEC/ (last access: 8 February 2023, kindly provided as a single ZIP file by Andrew MacDougall).

The decrease in excess CO_2 in the atmosphere and increases in the carbon stocks of the WO and the TB, subsequent to cessation of anthropogenic emissions, are all shown in Fig. 4a–c as a fraction f relative to the amount of excess CO_2 in the atmosphere at the time of cessation; all figures are at the same scale. The normalization to initial excess atmospheric CO_2, which accounts for differences among the models in the amount of excess atmospheric CO_2 at the time of cessation, permits comparison across the set of models of the apportionment of net transfer from the atmosphere (i.e., the decrease in f_A, from its initial value of unity) into the WO, f_O, and the TB, f_T. The differences in the stocks in the WO and the TB relative to their values at the time of cessation, initially zero, increase as a function of time subsequent to cessation, as excess atmospheric CO_2 present at the time of cessation is taken up by each of those compartments in the absence of further anthropogenic emissions (i.e., net zero anthropogenic emissions). This intercomparison is thus highly pertinent to a prospective transition to net zero emissions, in contrast to the J13 study, which is pertinent to the disposition of an amount of CO_2 emitted at a given time. Because of these different protocols the results of the two studies cannot be directly compared. Importantly, the initial changes in the stocks following the pulse emission, relative to the magnitude of the pulse (J13), are much greater than those following abrupt cessation of emissions, relative to the amount of excess atmospheric CO_2 at the time of cessation (M20).

For all the models excess atmospheric CO_2 began to decrease immediately upon cessation as excess atmospheric CO_2 was being drawn into the WO and the TB. All models showed a more or less monotonic decrease in atmospheric CO_2 throughout the initial 100 years subsequent to cessation; a few instances of temporary positive slope are indicative of a slight, short-term net increase in atmospheric CO_2. The fractional removal of excess atmospheric CO_2 at time subsequent to cessation $t = 100$ years ranged across the models from 26 % to 47 % (i.e., fraction of excess CO_2 remaining 53 % to 74 %). All but one of the models showed the net amount of

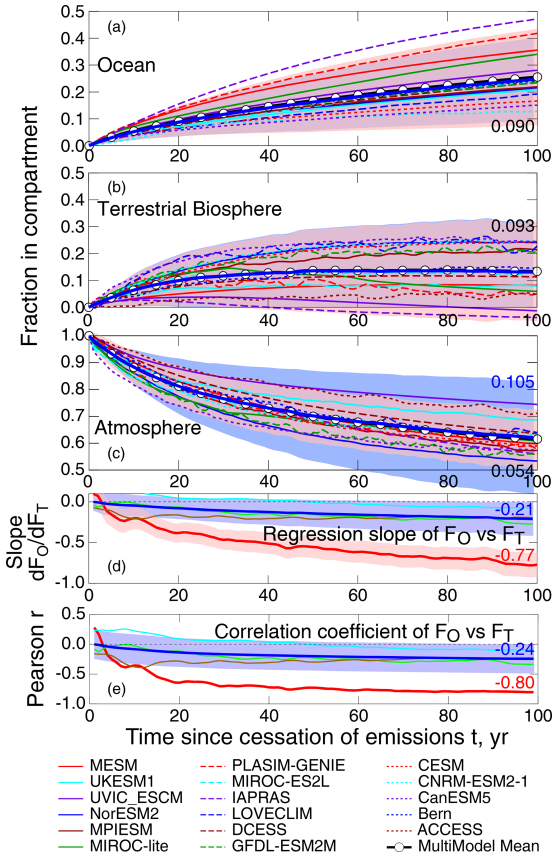

Figure 4. Time dependence of the fraction of excess atmospheric CO_2 (above its preindustrial level) at the time of cessation of anthropogenic emissions taken up by **(a)** the world ocean, **(b)** the terrestrial biosphere, and **(c)** the atmosphere, subsequent to abrupt cessation of emissions, f_O, f_T, and f_A, respectively, as calculated by the models that participated in the ZECMIP intercomparison (MacDougall et al., 2020, M20). For details on the intercomparison and identification of the participating models, see M20. Pink shading denotes ±2 SD about the multimodel mean; SDs at $t = 100$ years after cessation are in black text. Thick blue curve and blue shading denote mean and ±2 times the mean SD of 120 instances of IRFs calculated with randomly sorted pairs of net transfer coefficients (k_O, k_T) taken from the set of net transfer coefficients evaluated from the data presented by M20; violet shading denotes overlap of blue and pink shading as in Fig. 1. Mean SD for f_A at $t = 100$ years is in blue text. The three panels are to the same scale. **(d)** Regression slope of linear fit of time-dependent fraction of uptake into WO, f_O, vs. into TB, f_T; pink shading denotes ±1 SD; value at 100 years is in red text; the thick blue line denotes mean of regression slope of linear fit of f_O vs. f_T evaluated for 120 instances of randomly sorted pairs of net transfer coefficients (k_O, $k_{T,i}$) taken from the set of net transfer coefficients evaluated from the data presented by M20; blue shading denotes ±1 SD; the value at $t = 100$ years is in blue text; thin curves denote time series of regression slopes for three instances of such random pairings. **(e)** Pearson correlation coefficient r of linear regression of f_O vs. f_T for the several models is denoted by the thick red line; mean and ±1 SD of r, for 120 instances of k_O and k_T, are the thick blue lines, as in **(d)**; values at $t = 100$ years are as in **(d)**; thin curves denote correlation coefficients for three instances of those regressions.

CO_2 taken up by the WO increasing monotonically throughout the initial 100 years. All models also showed net uptake by the TB in the initial years subsequent to cessation but with larger inter-model variation than for net uptake by the WO. In contrast to ocean uptake, the increase in TB amount exhibited substantial fluctuations for almost all the models. For all the models, toward the end of the 100-year period, the amount of uptake by the TB either leveled off, decreased, or in some models actually became negative (cumulative transfer from the TB back into the atmosphere over the initial 100 years exceeding cumulative transfer from the atmosphere into the TB). The spread of the extent of transfer into the two individual compartments (0.090 and 0.093 at $t = 100$ years, 1 SD) was much greater than the spread in f_A (0.054). The fraction of the excess atmospheric CO_2 at the time of cessation taken up by the ocean at 100 years f_O (100 years) ranged across the models from 13 % to 47 %. The fractional uptake by the TB f_T (100 years) ranged from as great as about 25 % in three models to negative values in two models (i.e., stock in the TB actually decreasing over the time period, by 1 % or 4 % relative to the initial excess atmospheric CO_2).

As in the results from the J13 intercomparison, there is substantial anticorrelation across the suite of ZECMIP models between the extent of uptake into the WO and the TB. This is manifested in the first instance in the much narrower inter-model spread of the extent of decrease in the fraction of initial excess CO_2 remaining in the atmosphere than in the fractional uptake, again relative to the amount of excess atmospheric CO_2 at the time of cessation of anthropogenic emissions, by the ocean f_O and the terrestrial biosphere f_T. This anticorrelation is also manifested in the Pearson correlation coefficient, r, which is negative throughout almost the entire 100-year time period examined. The regression slope, initially rather small, increases (in magnitude) throughout the time period, almost to -0.8; a slope of -1 would indicate a one-to-one compensation between net uptake into the two compartments. This anticorrelation is also manifested in graphs of the net fractional uptake into the ocean versus that into the terrestrial biosphere, shown in Fig. 5a, at the end of the time period examined by M20, $t = 100$ years after cessation of anthropogenic emissions.

Again, as with the results from J13, the question arises of the contribution to the anticorrelation across the models in the extent of uptake of excess atmospheric CO_2 by the WO and the TB. To what extent is this due to competition between excess CO_2 taken up previously by one compartment reducing the amount available to be taken up by the other compartment? The contribution of this competition effect to the anticorrelation was first assessed by examining the net transfer coefficients, evaluated as the time-dependent rate of net increase in the fractional uptake into each of the two compartments divided by the time-dependent fraction of excess atmospheric CO_2, k_O, and k_T (Fig. 6). As the transfer rates and stocks were available from the Supplement and project website, it was not necessary to numerically differentiate the time-dependent stocks, as was done in the analysis of J13. In several models the transfer coefficients were highly variable over time, with especially large fluctuations in the net transfer coefficients into the TB (Fig. 6b) and in the fractional rate of decrease in excess atmospheric CO_2 (Fig. 6c), which is nominally the sum of the net transfer coefficients into the WO and the TB. Despite these large fluctuations, it was found that the regression slope and r value, evaluated for each year over the 100-year period following cessation, were both consistently negative, for almost every year in this time period. Importantly also, the correlation slope between k_O and k_T was negative throughout almost the entire time period. An example plot of k_O vs. k_T is shown in Fig. 5b, for time $t = 55$ years subsequent to cessation, a time period during which a fairly consistent negative correlation was exhibited (Fig. 6d and e). While a single plot with correlation coefficient -0.58 might not be convincing by itself, the consistent negative correlation between k_O and k_T would seem to make a fairly convincing case for negative correlation between these net transfer coefficients. Again, as was concluded for the models participating in the J13 intercomparison, such an anticorrelation would imply that models for which the terrestrial module resulted in relatively high uptake rate into the TB had an ocean module that resulted in relatively low uptake rate into the WO and vice versa. This anticorrelation between the transfer coefficients k_O and k_T resulted in substantial enhancement, by a factor of 3 or so, of anticorrelation of the net uptake extent into the two compartments in excess of that which would result only from the compensation effect as evaluated for random parings of k_O and k_T (Fig. 4d and e).

As with the analysis of J13, the cause of the anticorrelation extent of uptake into the WO and the TB was further assessed by calculations in which the transfer coefficients k_T of several models were randomly paired with the k_O's with examination of the resultant correlations between uptake by the WO and the TB and the corresponding transfer coefficients, for a total of 120 such random pairings. Again these random pairings exhibited essentially no correlation in the transfer coefficients themselves. The mean correlation slope b at 55 years after cessation was -0.01 ± 0.11 (1 SD; Fig. 6d), much less than the regression slope for the (k_O, k_T) pairs for the models, -0.22 ± 0.14. A similar situation was found for the correlation coefficient (Fig. 6e) r (55 years) $= 0.03 \pm 0.30$ vs. -0.58 for the (k_O, k_T) pairs for the models. Again there was meandering of the correlation coefficient of individual instances of pairing, three of which are shown in Fig. 6e. Some of the individual curves meandered considerably outside ± 1 SD, which is of course to be expected, but none exhibited the systematic strong anticorrelation exhibited by IRFs of the models, as shown by the thick red curve.

The anticorrelation of the transfer coefficients was found to exert quite a substantial influence on the anticorrelation of the extent of transfer (Fig. 4). In Fig. 4a–c, the curves for the original models and the associated spread, the pink-shaded

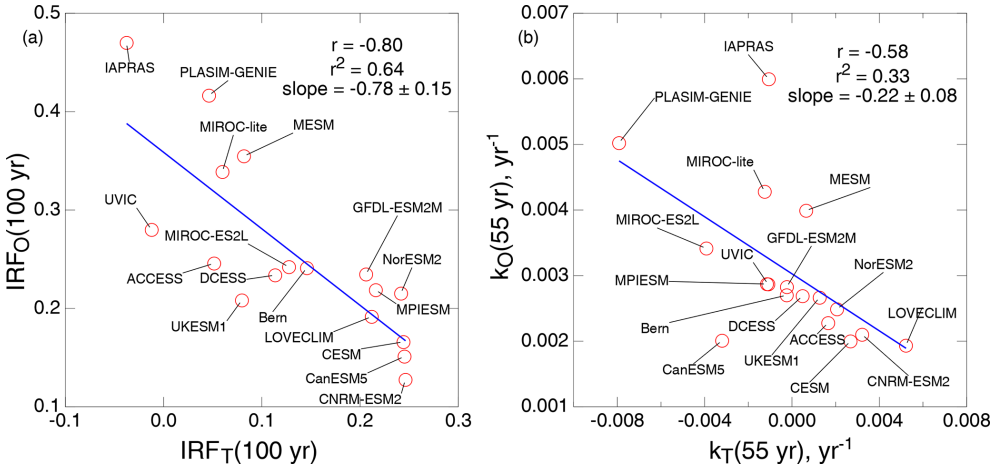

Figure 5. **(a)** Net uptake of CO_2 in the world ocean IRF(WO) versus that in the terrestrial biosphere IRF(TB), both expressed as fraction of excess atmospheric CO_2 (i.e., above its preindustrial level) at the time of cessation of emissions, at time $t = 100$ years subsequent to cessation of anthropogenic emissions, as represented by the models that participated in the ZECMIP intercomparison study of MacDougall et al. (2020, M20); negative values for IRF(TB) denote net cumulative decrease in carbon stock in the TB over the 100-year time period. The blue line denotes linear regression; also shown are the regression slope, the Pearson correlation coefficient r, and r^2. For identification of models, see M20. **(b)** As in **(a)** but for transfer coefficient for net uptake of excess atmospheric CO_2 from the atmosphere to the WO k_O versus that from the atmosphere to the TB k_T at time $t = 55$ years; negative values of k_T denote net transfer from the TB to the atmosphere at that time.

region, represent ± 2 SD of the fraction of the excess atmospheric CO_2 at the time of cessation of anthropogenic emissions that is transferred into the WO or the TB, and the fraction remaining in the atmosphere. These curves are superimposed on the averages taken over 120 random pairings of k_O and k_T, thick blue line (and averages of 2 SD, blue shading). For transfer extents f_O and f_T, the range of the blue shading (randomized pairs (k_O, $k_{T,i}$)) is essentially the same as that of the pink shading (models). However for the fractional extent of removal from the atmosphere f_A, while the curve that represents the mean of the 120 instances of random (k_O, k_T) pairs (dark blue; no vertical adjustment, as was required in Fig. 1, is required here, because the time series started at $t = 0$) is virtually identical to that for the mean of the models themselves (black with open circles), the spread of f_A for the randomly paired k_O and k_T (blue shading) substantially exceeds that for the models themselves (pink shading), by nearly a factor of 2 by the end of the model runs. The difference between the blue-shaded area (spread of the randomized pairs (k_O, $k_{T,i}$)) and the pink-shaded area (spread of the models themselves) is a measure of the decrease in f_A that is due to anticorrelation of the transfer coefficients in the models. The effect of anticorrelation in the transfer coefficients is seen also in the regression slope b of f_O vs. f_T, -0.77 ± 0.15 for the models themselves vs. -0.21 ± 0.21 for the randomized pairs (k_O, $k_{T,i}$), Fig. 4d, and in the correlation coefficient r, -0.80 for the models vs. -0.24 for the randomized pairs, Fig. 4e (all at 100 years after cessation of anthropogenic emissions). Again, values of b and r for individual random (k_O, k_T) pairs meander more or less within the space of ± 1 SD, but this meandering is much less than the separation between the mean quantities for the randomized pairs and the values for the models.

3 Discussion

The intent of this study has been to determine, for the two model intercomparison studies under examination, J13 and M20, the extent and causes of anticorrelation across the models participating in each study in the net uptake of excess CO_2 by the WO and the TB under the experimental protocols of the two studies. The present analysis has demonstrated and quantified anticorrelation across the models that participated in each of the two intercomparison studies between the transfer coefficients characterizing the net rate of transport of excess atmospheric CO_2 into the two receiving compartments, the WO and the TB, subsequent to the pulse emission (J13) or to cessation of anthropogenic emissions (M20). This study has also, for each of the two studies examined, quantified the enhancement in anticorrelation in the extent of uptake in the two receiving compartments beyond that which would be expected inevitably from the competition effect alone and the resultant decrease in inter-model diversity.

The present study assessed anticorrelation across each of the model sets not only in the net uptake extent but also in the net transfer coefficients. The net transfer coefficient is defined as the time-dependent rate of transfer into the WO and TB divided by the time-dependent amount of atmospheric CO_2, for J13, in excess of the amount atmospheric CO_2, subsequent to the pulse, which would have been present in the

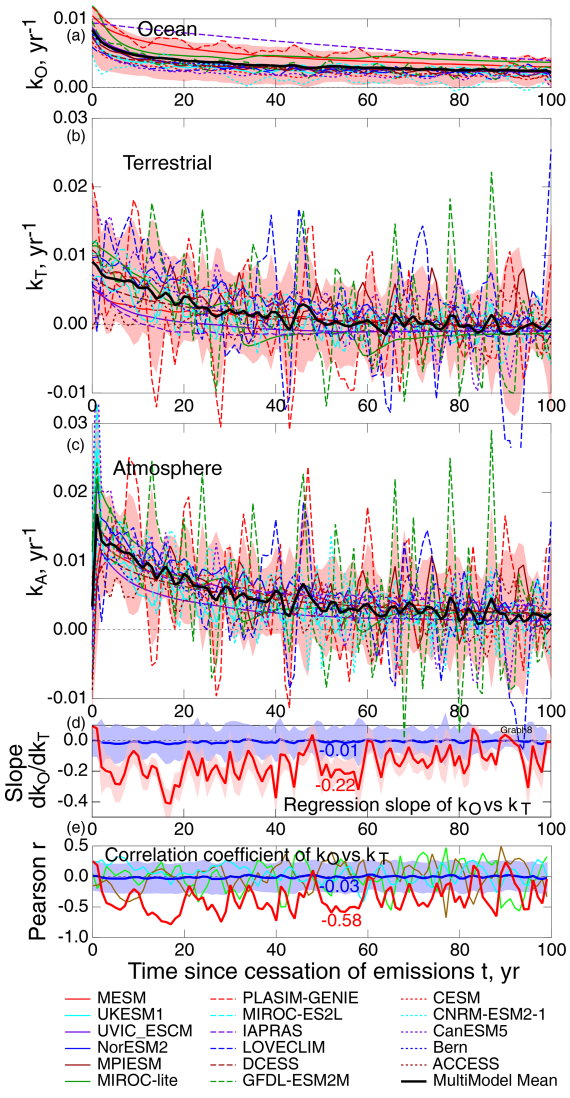

Figure 6. Net transfer coefficients from the atmosphere into **(a)** the world ocean k_O and **(b)** the terrestrial biosphere k_T as a function of time subsequent to cessation of emission of anthropogenic CO_2 into the atmosphere, evaluated from the results presented by MacDougall et al. (2020; M20); similarly, **(c)** denotes the fractional rate of decrease in excess CO_2 stock in the atmosphere. Pink shading denotes ± 2 SD about the multimodel mean; the three panels are to the same scale. For identification of the participating models, see M20. **(d)** Regression slope (thick red line) of the linear fit of k_O vs. k_T for the several models for each year over the 100-year period subsequent to cessation of emissions (see Fig. 5b for example), with the value at 55 years is indicated; shading denotes ± 1 SD; mean regression slope is denoted by a thick blue line, and ± 1 SD is denoted by blue shading, for 120 instances of k_O and k_T of different models being randomly paired, with the mean value at 55 years indicated; thin curves denote time series of three instances of those regression coefficients. **(e)** Pearson correlation coefficient r of linear regression of k_O vs. k_T for the several models (thick red line), with the value at 55 years is indicated; blue and blue shading are the mean and ± 1 SD of r, for the 120 instances of random pairing, with the mean value at 55 years indicated; thin curves denote time series of three instances of those correlation coefficients.

absence of the pulse, and for M20, in excess of preindustrial CO_2 subsequent to cessation of anthropogenic emissions. As these net transfer coefficients are not dependent on prior uptake, they are not subject to what is denoted here as the competition effect such that if more CO_2 has previously been taken up by one sink compartment, there is inevitably less available to be taken up by the other. In both studies significant anticorrelation was found between the transfer coefficients across the sets of participating models and that, as a consequence, diminished inter-model variance in the time-dependent extent of drawdown of excess atmospheric CO_2 relative to that which would be expected in the absence of anticorrelation in the transfer coefficients.

The transfer coefficients k_O and k_T, being based on the net transfer rates, and the extents of transfer, being the integrals of the transfer rates, are net quantities, the difference between fluxes in the opposing directions. (As k_A is not a transfer coefficient per se but represents the total net flux, from the atmosphere to the WO and the TB, again normalized to excess atmospheric CO_2, fluctuations in k_A simply represent the sum of fluctuations in k_O and k_T, which must be considered more fundamental than those in k_A.) In both studies examined here fluctuations in k_T greatly exceeded those in k_O (and thus dominated fluctuation in k_A). It would seem almost certain that the large interannual fluctuations in k_T in several of the models arise from externally imposed influences in processes controlling this net uptake such as temperature, cloudiness, precipitation, and fire, which seemingly are built into the models, or into the parent climate models, to represent variability in these processes and to examine the consequences of this variability, as opposed to processes that would actually occur in a given hypothetical future year subsequent to the pulse emission or cessation of emissions. From an observational perspective, some sense of the temporal variability of the global rate of net drawdown of atmospheric CO_2 is gained from the historical time series of fractional annual removal rate of excess CO_2, corresponding to k_A, which has ranged, over the time period 1959–2012, from as great as 4.3 % yr^{-1} to as low as 0.8 % yr^{-1} but never negative (Raupach et al., 2014). It would thus seem that some of the models may be overestimating the effects of climate variables on the rate of drawdown of excess CO_2 in future climate, perhaps substantially so. In any event, given the large intra-model and inter-model fluctuations in k_T, it came as rather a surprise in this analysis to be able to demonstrate and quantify consistently negative inter-model anticorrelation between k_O and k_T across the models that participated in each of the studies.

The finding of inter-model anticorrelation between k_O and k_T led to determination of effect of this anticorrelation on enhancement of anticorrelation in the time-dependent extent of transfer of excess CO_2 into the two receiving compartments. Here the term "enhancement" is introduced to account for anticorrelation greater than that which would inevitably arise from the competition effect. A method was introduced

to estimate the competition effect by randomizing the time-dependent pairs of net transfer coefficients. From comparison of the results from the model intercomparisons with those for the randomized (k_O, k_T) pairs, it was shown by the several measures of anticorrelation examined here that, in the each of the two studies, the anticorrelation between the amount of excess atmospheric taken up by the WO and the TB well exceeds that due to the competition effect, leading to substantial underestimation of the inter-model diversity that had previously been inferred from these studies.

Inter-model diversity of a quantity of interest may confidently be taken as a measure of the minimum uncertainty that would attach to knowledge of that quantity, at least as represented by the set of models examined. Not uncommonly, however, inter-model diversity is *equated* with uncertainty, e.g., in the present context, by Joos et al. (2013), and by the IPCC Fifth Assessment Report (Myhre et al., 2013). The finding here of substantial underestimation of inter-model diversity in the time-dependent extent of drawdown of excess atmospheric CO_2 implies a greater uncertainty in key measures of drawdown than has previously been recognized and ascribed to this quantity.

From a cumulative forcing perspective, the pertinent quantity is not the atmospheric IRF but its integral over the time horizon of interest. This integrated IRF, shown for the pulse emission study of J13 in their Fig. 1b, is equal to 52.4 years for the J13 multimodel mean, with a standard deviation of 5.5 years (10 %). The difference between the violet and blue regions of Fig. 1c is the reduction in inter-model diversity (expressed as ± 2 SD) due to anticorrelation of the transfer coefficients across the models. From integration of the upper and lower bounds of the blue-shaded region in Fig. 1c, which gives the ± 2 SD range of the spread in IRFs that would result only from the competition effect, which is in the absence of anticorrelation of the transfer coefficients across the models, the standard deviation of the integrated IRF increases to 8.1 years (15 %), an increase of about 50 %. This increase in inter-model diversity would attach also to the absolute global warming potential (AGWP) of CO_2, defined as the cumulative atmospheric IRF of CO_2 times its forcing efficiency, a quantity widely used in assessments, such as the IPCC Fifth Assessment Report (Myhre et al., 2013, p. 712), of the cumulative effects of prospective changes in emissions of CO_2.

The AGWP of CO_2 is also widely used to compare the integrated radiative forcings of non-CO_2 greenhouse gases (NCGHGs) to that of CO_2 via the global warming potential (GWP), the ratio of AGWP of NCGHGs to that of CO_2. In the IPCC Fifth Assessment Report, Myhre et al. (2013) state that the GWP has become the "default metric" for transferring emissions of different gases to a common scale, CO_2-equivalent emissions, also observing that the GWP for a time horizon of 100 years has been adopted as a metric to implement a multi-gas approach to achieve specific targets. The increase in inter-model spread of the cumulative atmospheric IRF resulting from the present analysis also attaches to the GWPs and to equivalent emissions of NCGHGs, affecting the confidence that can be placed in strategies to achieve specific targets and the confidence that can be placed in replacing emissions of one GHG with another in achieving target GHG emissions. For all these reasons it seems essential that the minimum uncertainty in rate of drawdown of excess CO_2, as represented by inter-model diversity, be accurately known and stated. If the inter-model diversity in integrated IRFs obtained here is an accurate characterization of the uncertainty in that quantity, then the uncertainties in the AGWP of CO_2 and in the GWPs of NCGHGs would increase by a similar amount.

A question that naturally arises is the reason for the anticorrelation in drawdown rates across the sets of models participating in the two studies. A similar situation of anticorrelation across nominally independent models was found to exist between modeled climate sensitivity, forcing, and temperature change over the industrial era, as reported in a suite of climate model studies. This situation was initially identified (Schwartz et al., 2007) from the inter-model diversity in temperature change in climate model studies being much less than the uncertainty in forcing. Shortly afterwards Kiehl (2007) showed that this was due to inverse correlation across the set of models between forcing and climate sensitivity. Reflecting on such anticorrelation across nominally independent models, Sherwood et al. (2020) underscore the need to identify model co-dependencies that might have the effect of diminishing uncertainty in estimates of climate sensitivity. Sherwood et al. (2020) observe that "Modelers and process experts are aware of the historical climate record. GCM [general circulation model] aerosol forcings might have been selected in order to match the observed warming rate over the 20th century (e.g., Kiehl, 2007)." Sherwood et al. (2020) go onto suggest that "otherwise plausible models or feedbacks might have been discarded because of perceived conflict with this warming rate, or aversion to a model's climate sensitivity being outside an accepted range."

It would seem that considerations such as these might apply similarly to the anticorrelation in the modeled rate of drawdown of excess CO_2 subsequent to pulse emission (J13) or following abrupt cessation of anthropogenic emissions (M20). A sine qua non in modeling atmospheric CO_2 over the industrial period is that the model accurately represents the observed increase in atmospheric CO_2 over this period. This requirement, together with historical emissions, fixes the total time-dependent rate of net drawdown of excess atmospheric CO_2, which is the sum of the net drawdown rates into the ocean and the TB. Thus to meet this observational constraint, if the net transfer rate from the atmosphere into one compartment is high, the net transfer rate into the other must be low. This requirement, built into CO_2 models because of the requirement that they accurately represent atmospheric CO_2 in historical runs, might plausibly lead to the anticorrelation of net uptake rates into the two compartments that is revealed in the present analysis of model responses to

artificial emission scenarios in the two studies under examination. I thank Andrew MacDougall in his capacity as reviewer of this paper (MacDougall, 2024) for stimulating my thoughts along these lines.

At the end of the day this study has done little to identify the underlying causes of the observed anticorrelations. Identifying these causes would, it would seem, require a much more thorough examination of the representations of the processes governing net uptake of excess atmospheric CO_2 into the two receiving compartments than can be achieved simply by intercomparisons of rate and extent of drawdown such as in the two studies examined here. Nonetheless it would seem that if progress is to be made in representing these processes and in enhancing confidence in these representations, such a thorough inter-model comparison at the process level is required.

For the present, at minimum, it would seem incumbent upon the communities using the results of these intercomparison studies to assess the consequences of prospective changes in emissions or to compare integrated forcings of CO_2 and other greenhouse gases to take cognizance of the implications of anticorrelations across the models participating in the two intercomparison studies examined here and resultant artificial decrease in inter-model diversity in these two studies.

Data availability. Data from the ZECMIP project (MacDougall et al., 2020) are available from http://terra.seos.uvic.ca/ZEC/. Data from the Joos et al. (2013) intercomparison were obtained by digitization of the figures in the published paper; available also at https://climatehomes.unibe.ch/~joos/IRF_Intercomparison/. Data displayed in the figures are presented in Supplement.

Supplement. The supplement related to this article is available online at: https://doi.org/10.5194/bg-21-5045-2024-supplement.

Competing interests. The author has declared that there are no competing interests.

Disclaimer. Views expressed here are those of the author and do not necessarily reflect the views of Brookhaven National Laboratory or the U.S. Department of Energy.

Acknowledgements. I thank Andrew MacDougall for providing the M20 data, for discussion, and for valuable suggestions in his capacity as reviewer of the manuscript. I also thank Lawrence Kleinman and Ernie Lewis and one anonymous reviewer for valuable suggestions. Much of this work was conducted while the author was at the Brookhaven National Laboratory, with support in part from the U.S. Department of Energy (contract no. DE-SC0012704).

Financial support. This research has been supported by the U.S. Department of Energy (grant no. DE-SC0012704).

Review statement. This paper was edited by Paul Stoy and reviewed by Andrew MacDougall and one anonymous referee.

References

Bacastow, R. and Keeling, C. D.: Atmospheric carbon dioxide and radiocarbon in the natural carbon cycle. II. Changes from AD 1700 to 2070 as deduced from a geochemical model, in: Carbon and the Biosphere, edited by: Woodwell, G. M. and Pecan, E. V., U. S. Atomic Energy Commission Report CONF-720510, OSTI Identifier, 4380392, 86–135, 1973.

Friedlingstein, P., O'Sullivan, M., Jones, M. W., Andrew, R. M., Gregor, L., Hauck, J., Le Quéré, C., Luijkx, I. T., Olsen, A., Peters, G. P., Peters, W., Pongratz, J., Schwingshackl, C., Sitch, S., Canadell, J. G., Ciais, P., Jackson, R. B., Alin, S. R., Alkama, R., Arneth, A., Arora, V. K., Bates, N. R., Becker, M., Bellouin, N., Bittig, H. C., Bopp, L., Chevallier, F., Chini, L. P., Cronin, M., Evans, W., Falk, S., Feely, R. A., Gasser, T., Gehlen, M., Gkritzalis, T., Gloege, L., Grassi, G., Gruber, N., Gürses, Ö., Harris, I., Hefner, M., Houghton, R. A., Hurtt, G. C., Iida, Y., Ilyina, T., Jain, A. K., Jersild, A., Kadono, K., Kato, E., Kennedy, D., Klein Goldewijk, K., Knauer, J., Korsbakken, J. I., Landschützer, P., Lefèvre, N., Lindsay, K., Liu, J., Liu, Z., Marland, G., Mayot, N., McGrath, M. J., Metzl, N., Monacci, N. M., Munro, D. R., Nakaoka, S.-I., Niwa, Y., O'Brien, K., Ono, T., Palmer, P. I., Pan, N., Pierrot, D., Pocock, K., Poulter, B., Resplandy, L., Robertson, E., Rödenbeck, C., Rodriguez, C., Rosan, T. M., Schwinger, J., Séférian, R., Shutler, J. D., Skjelvan, I., Steinhoff, T., Sun, Q., Sutton, A. J., Sweeney, C., Takao, S., Tanhua, T., Tans, P. P., Tian, X., Tian, H., Tilbrook, B., Tsujino, H., Tubiello, F., van der Werf, G. R., Walker, A. P., Wanninkhof, R., Whitehead, C., Willstrand Wranne, A., Wright, R., Yuan, W., Yue, C., Yue, X., Zaehle, S., Zeng, J., and Zheng, B.: Global Carbon Budget 2022, Earth Syst. Sci. Data, 14, 4811–4900, https://doi.org/10.5194/essd-14-4811-2022, 2022.

Joos, F., Roth, R., Fuglestvedt, J. S., Peters, G. P., Enting, I. G., von Bloh, W., Brovkin, V., Burke, E. J., Eby, M., Edwards, N. R., Friedrich, T., Frölicher, T. L., Halloran, P. R., Holden, P. B., Jones, C., Kleinen, T., Mackenzie, F. T., Matsumoto, K., Meinshausen, M., Plattner, G.-K., Reisinger, A., Segschneider, J., Shaffer, G., Steinacher, M., Strassmann, K., Tanaka, K., Timmermann, A., and Weaver, A. J.: Carbon dioxide and climate impulse response functions for the computation of greenhouse gas metrics: a multi-model analysis, Atmos. Chem. Phys., 13, 2793–2825, https://doi.org/10.5194/acp-13-

2793-2013, 2013 (data available at: https://climatehomes.unibe.ch/~joos/IRF_Intercomparison/, last access: 31 October 2024).

Kiehl, J. T.: Twentieth century climate model response and climate sensitivity, Geophys. Res. Lett., 34, L22710, https://doi.org/10.1029/2007GL031383, 2007.

MacDougall, A.: Referee Comment 1, Comment on egusphere-2024-748, https://doi.org/10.5194/egusphere-2024-748#RC1, 2024.

MacDougall, A. H., Frölicher, T. L., Jones, C. D., Rogelj, J., Matthews, H. D., Zickfeld, K., Arora, V. K., Barrett, N. J., Brovkin, V., Burger, F. A., Eby, M., Eliseev, A. V., Hajima, T., Holden, P. B., Jeltsch-Thömmes, A., Koven, C., Mengis, N., Menviel, L., Michou, M., Mokhov, I. I., Oka, A., Schwinger, J., Séférian, R., Shaffer, G., Sokolov, A., Tachiiri, K., Tjiputra, J., Wiltshire, A., and Ziehn, T.: Is there warming in the pipeline? A multi-model analysis of the Zero Emissions Commitment from CO_2, Biogeosciences, 17, 2987–3016, https://doi.org/10.5194/bg-17-2987-2020, 2020 (data available at: http://terra.seos.uvic.ca/ZEC/, last access: 8 February 2023).

Millar, R. J., Nicholls, Z. R., Friedlingstein, P., and Allen, M. R.: A modified impulse-response representation of the global near-surface air temperature and atmospheric concentration response to carbon dioxide emissions, Atmos. Chem. Phys., 17, 7213–7228, https://doi.org/10.5194/acp-17-7213-2017, 2017.

Myhre, G., Shindell, D., Bréon, F.-M., Collins, W., Fuglestvedt, J., Huang, J., Koch, D., Lamarque, J.-F., Lee, D., Mendoza, B., Nakajima, T., Robock, A., Stephens, G., Takemura, T., and Zhang, H.: Anthropogenic and Natural Radiative Forcing, in: Climate Change 2013: The Physical Science Basis, Contribution of Working Group I to the Fifth Assessment Report of the Intergovernmental Panel on Climate Change, edited by: Stocker, T. F., Qin, D., Plattner, G.-K., Tignor, M., Allen, S. K., Boschung, J., Nauels, A., Xia, Y., Bex, V., and Midgley, P. M., Cambridge University Press, Cambridge, United Kingdom and New York, NY, USA, https://doi.org/10.1017/CBO9781107415324.018, 2013.

Press, W. H., Teukolsky, S. A., Vetterling, W. T., and Flannery, B. P.: Numerical Recipes in C, 2nd Edn., Cambridge University Press, Section 15.2, ISBN 0-521-43108-5, 1997.

Raupach, M. R., Gloor, M., Sarmiento, J. L., Canadell, J. G., Frölicher, T. L., Gasser, T., Houghton, R. A., Le Quéré, C., and Trudinger, C. M.: The declining uptake rate of atmospheric CO_2 by land and ocean sinks, Biogeosciences, 11, 3453–3475, https://doi.org/10.5194/bg-11-3453-2014, 2014.

Schwartz, S. E., Charlson, R. J., and Rodhe, H.: Quantifying climate change – too rosy a picture?, Nature Reports Climate Change, 2, 23–24, 2007.

Sherwood, S. C., Webb, M. J., Annan, J. D., Armour, K. C., Forster, P. M., Hargreaves, J. C., Hegerl, G., Klein, S. A., Marvel, K. D., Rohling, E. J., Watanabe, M., Andrews, T., Braconnot, P., Bretherton, C. S., Foster, G. L., Hausfather, Z., von der Heydt, A. S., Knutti, R., Mauritsen, T., Norris, J. R., Proistosescu, C., Rugenstein, M., Schmidt, G. A., Tokarska, K. B., and Zelinka, M. D.: An assessment of Earth's climate sensitivity using multiple lines of evidence, Rev. Geophys., 58, e2019RG000678, https://doi.org/10.1029/2019RG000678, 2020.

Smith, C. J., Forster, P. M., Allen, M., Leach, N., Millar, R. J., Passerello, G. A., and Regayre, L. A.: FAIR v1.3: a simple emissions-based impulse response and carbon cycle model, Geosci. Model Dev., 11, 2273–2297, https://doi.org/10.5194/gmd-11-2273-2018, 2018.